Combined mTORC1/mTORC2 inhibition blocks growth and induces catastrophic macropinocytosis in cancer cells

Ritesh K. Srivastava[a], Changzhao Li[a], Jasim Khan[a], Nilam Sanjib Banerjee[b], Louise T. Chow[b,1], and Mohammad Athar[a,1]

[a]Department of Dermatology, University of Alabama at Birmingham, Birmingham, AL 35294; and [b]Department of Biochemistry and Molecular Genetics, University of Alabama at Birmingham, Birmingham, AL 35294

Contributed by Louise T. Chow, October 4, 2019 (sent for review July 3, 2019; reviewed by Hasan Mukhtar and Brian A. Van Tine)

The mammalian target of rapamycin (mTOR) pathway, which plays a critical role in regulating cellular growth and metabolism, is aberrantly regulated in the pathogenesis of a variety of neoplasms. Here we demonstrate that dual mTORC1/mTORC2 inhibitors OSI-027 and PP242 cause catastrophic macropinocytosis in rhabdomyosarcoma (RMS) cells and cancers of the skin, breast, lung, and cervix, whereas the effects are much less pronounced in immortalized human keratinocytes. Using RMS as a model, we characterize in detail the mechanism of macropinocytosis induction. Macropinosomes are distinct from endocytic vesicles and autophagosomes in that they are single-membrane bound vacuoles formed by projection, ruffling, and contraction of plasma membranes. They are positive for EEA-1 and LAMP-1 and contain watery fluid but not organelles. The vacuoles then merge and rupture, killing the cells. We confirmed the inhibition of mTORC1/mTORC2 as the underpinning mechanism for macropinocytosis. Exposure to rapamycin, an mTORC1 inhibitor, or mTORC2 knockdown alone had little or reduced effect relative to the combination. We further demonstrate that macropinocytosis depends on MKK4 activated by elevated reactive oxygen species. In a murine xenograft model, OSI-027 reduced RMS tumor growth. Molecular characterization of the residual tumors was consistent with the induction of macropinocytosis. Furthermore, relative to the control xenograft tumors, the residual tumors manifested reduced expression of cell proliferation markers and proteins that drive the epithelial mesenchymal transition. These data indicate a role of mTORC2 in regulating tumor growth by macropinocytosis and suggest that dual inhibitors could help block refractory or recurrent RMS and perhaps other neoplasms and other cancer as well.

mTORC1/2 inhibitors | macropinocytosis | rhabdomyosarcoma cell lines | RMS xenografts | EMT

In addition to apoptosis, several other forms of cell death have been described, including autophagy-associated cell death, paraptosis, oncosis, necrosis, entosis, and macropinocytosis (1, 2). Among them, macropinocytosis has been shown to be an important cell death-associated process but only in limited cancer cell lines, such as neuroblastoma, glioblastoma, and colorectal cancer (1, 3–5). This form of cell death is characterized by the formation of plasma membrane ruffles or lamellipodia. The ruffle fuses with the plasma membrane enclosing the extracellular fluid, generating vesicles called macropinosomes that are heterogeneous in shape and size. An important feature that distinguishes macropinosomes from other endocytic vesicles is a rapid incorporation of fluid-phase tracers, such as fluorescent dextrans and lucifer yellow (LY) (6, 7).

Mammalian target of rapamycin (mTOR) signaling pathways regulate various cellular processes, including protein translation, growth, proliferation, angiogenesis, autophagy, stress response, and survival (8). mTOR comprises the catalytic subunits of 2 structurally and functionally different protein complexes, mTOR complex 1 (mTORC1) and mTOR complex 2 (mTORC2). The complexes are identified by unique regulatory proteins, namely Raptor (regulatory-associated protein of mTOR) for mTORC1 and Rictor (rapamycin-insensitive companion of mTOR) for mTORC2 (9). Aberrant activation of these components of mTOR signaling pathways is associated with many cancer types, including those that develop in the skin, lung, colon, breast, and brain (10–12).

Recently, we and others have reported an association of mTOR up-regulation with rhabdomyosarcoma (RMS) tumor progression (13, 14). Although mTORC1 inhibitors initially exhibited some inhibitory effects, the tumors became resistant due to feedback activation of AKT signaling by the mTORC2-regulated phosphorylation (15). Therefore, extensive efforts are now ongoing to develop potent inhibitors that could simultaneously target both mTORC1 and mTORC2 signaling pathways (16, 17). These inhibitors have been shown to be more effective than rapalogs in suppressing protein synthesis and tumor growth (18).

In this study, we observed that the dual mTORC1 and mTORC2 inhibitors induced extensive lethal vacuoles consistent with macropinosomes in RMS and in cancer cell lines of skin, breast, lung, and cervix. Understanding the signaling pathways underlying macropinocytosis-associated cell death is an important step in developing additional effective strategies to treat neoplasms that are resistant to apoptosis induced by chemotherapy. Using RMS cells as a model, we describe an important mechanism by which the dual inhibitor induces macropinocytosis. We confirm the roles of both mTOR complexes in controlling macropinocytosis by showing that rapamycin, an mTORC1 inhibitor (18), had little effect but increased macropinosomes induced by mTORC2 knockdown. mTORC1/2 inhibitor OSI-027–treated and PP242-treated cells developed numerous vacuoles that rapidly incorporated liquid-phase tracer LY and were positive for late

Significance

We report that cell lines of rhabdomyosarcoma (RMS) and cancer cell lines of skin, breast, lung, and cervix are highly sensitive to mTORC1/2 dual inhibitors. mTORC1/2 complexes regulate protein synthesis, cell proliferation, growth, stress responses and survival. The cancer cells died by a catastrophic process, called macropinocytosis, in which numerous single-membrane vacuoles filled with watery fluid formed, merged, and ruptured, killing the cells. Consistent with the findings in cultured cells, the growth of RMS cells implanted in immunocompromised mice was significantly reduced, especially in combination with cyclophosphamide, a standard chemotherapeutic drug to treat RMS.

Author contributions: R.K.S., L.T.C., and M.A. designed research; R.K.S., C.L., J.K., and N.S.B. performed research; R.K.S., C.L., L.T.C., and M.A. analyzed data; and R.K.S., L.T.C., and M.A. wrote the paper.

Reviewers: H.M., University of Wisconsin; and B.A.V.T., Washington University in St. Louis.

The authors declare no competing interest.

Published under the PNAS license.

[1]To whom correspondence may be addressed. Email: ltchow@uab.edu or mohammadathar@uabmc.edu.

This article contains supporting information online at https://www.pnas.org/lookup/suppl/doi:10.1073/pnas.1911393116/-/DCSupplemental.

First published November 15, 2019.

endosomal marker lysosomal-associated membrane protein 1 (LAMP-1) (19), the early endosome antigen 1 (EEA1) (20), and Ras-related protein Rab-5A (Rab5). We found that cell death was not mediated by apoptosis, autophagy, or inappropriate activation of Ras/Rac1; rather, MKK4 activated by elevated reactive oxygen species (ROS) played a critical role.

We also examined the effects of OSI-027 in RMS cell-derived xenograft tumors in athymic mice. The inhibitors were effective in reducing tumor growth, especially when tested in combination with cyclophosphamide, a chemotherapeutic agent commonly used in the standard care of a variety of cancers. We suggest that antitumor effects of OSI-027 are macropinocytosis-dependent, as revealed by the positive staining of residual tumor cells for LAMP-1 and EEA1. The residual tumor cells also displayed reduced biomarkers, characteristic of epithelium-to-mesenchymal transition.

In summary, using RMS as a model neoplasm, we investigated in-depth molecular underpinning of macropinocytosis induced by dual mTORC1/mTORC2 inhibitors. Our study also suggests that the dual inhibitors can enhance the efficacy of conventional chemotherapeutic agents in treating resistant cancers.

Results

OSI-027 and PP242 Induce Extensive Vacuolization in RMS and a Wide Range of Human Cancer Cell Lines. The antiproliferative effect of the dual mTORC1/mTORC2 inhibitors OSI-027 and PP242 has been documented in tumor cells derived from hepatocellular carcinoma, non–small-cell lung cancer, colon cancer, soft tissue sarcoma, ovarian cancer, etc., both in vitro and in xenograft mouse models (17, 18, 21–25). They inhibit phosphorylation of the mTORC1 substrates 4E-BP1 and S6K1 as well as the mTORC2 substrate AKT (17, 21). Interestingly, we noted that the dual inhibitors induced severe vacuolization in RD and RH30 cells, which represent 2 major RMS subtypes, embryonal (e) RMS and alveolar (a) RMS, respectively. We documented a robust time-dependent and concentration-dependent cytoplasmic vacuolization (Fig. 1*A* and *SI Appendix*, Fig. S1 *A* and *C*, *Movie*). Similar results were observed with 2 additional cell lines corresponding to eRMS and aRMS: SMS-CTR and CW9019, respectively (*SI Appendix*, Fig. S1*B*). These changes appear to be macropinocytosis, which has previously been described mainly in brain and colorectal cancer cell lines (4, 5).

Similarly, the dual inhibitors also induced cytoplasmic vacuolization in human cervical cancer cells (HeLa), human breast adenocarcinoma cells (MCF7), and human lung adenocarcinoma epithelial cells (A549) (Fig. 1*B*) in a concentration-dependent manner. In contrast, the changes in immortalized keratinocytes HaCaT and Ker-CT were less pronounced compared with those in human epidermoid carcinoma (A431) cells (Fig. 1 *C* and *D*). To investigate the nature of these vacuoles and mechanisms of induction, we concentrated on RMS cells in further studies.

Transmission Electron Microscopy Reveals Phenotypic Changes in OSI-027–Treated RMS Cells. After 24 h of exposure, more than 70% to 80% of RD or RH30 cells treated with OSI-027 or PP242 were positive for these cytoplasmic vacuoles that varied between 0.5 and 6.0 μm in diameter (Fig. 2*A* and *SI Appendix*, Fig. S2 *A* and *B*).

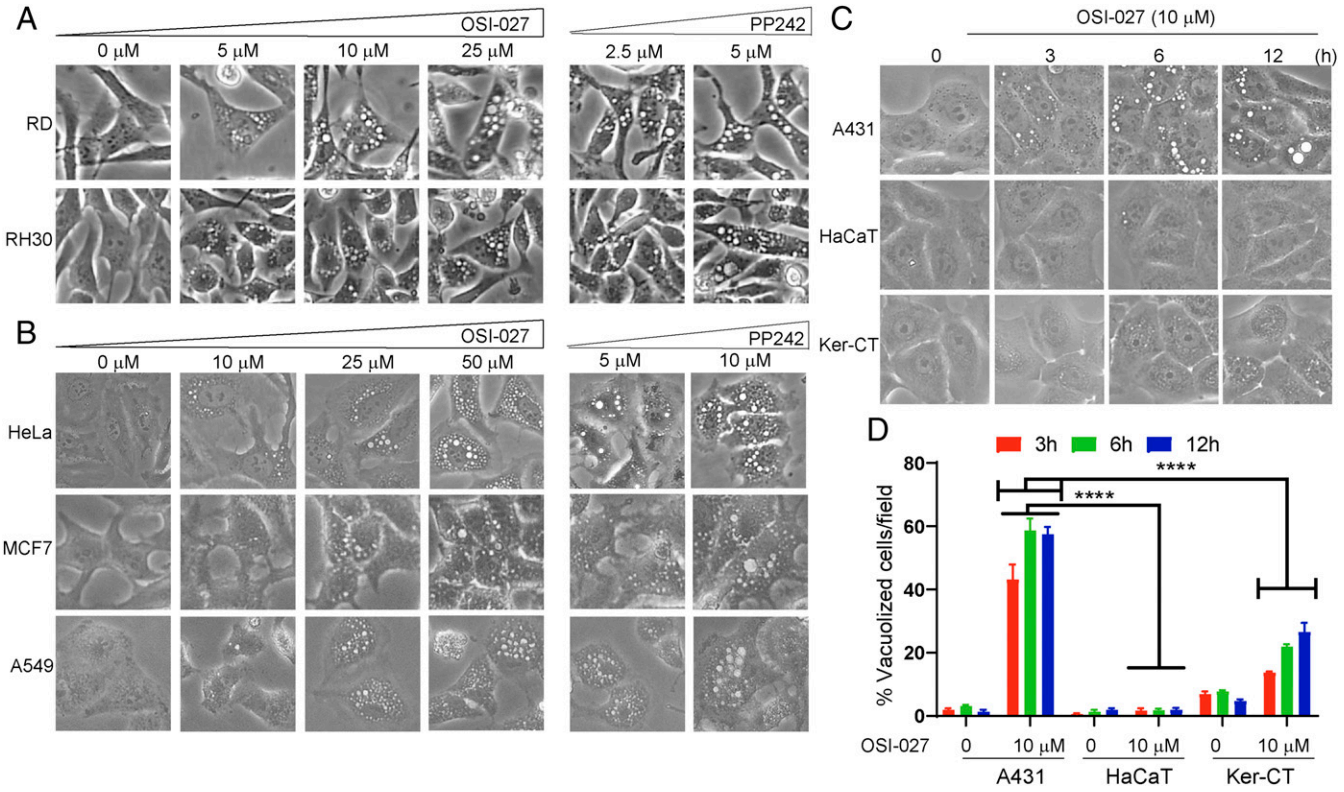

Fig. 1. Dual mTORC1/2 inhibitors induce extreme cytoplasmic vacuolization in diverse cancer cell lines. (*A*) Phase-contrast images showing dose-dependent effects on cytoplasmic vacuolization of RD and RH30 cells following OSI-027 (0 to 25 μM, 24 h) and PP242 (2.5 and 5 μM, 24 h) treatment. (*B*) Dose-dependent effects of OSI-027 (0 to 50 μM, 24 h) and PP242 (5 and 10 μM, 24 h) on human cervical cancer (HeLa), human breast adenocarcinoma (MCF7), and human lung adenocarcinoma (A549) cells. (*C*) Effects of OSI-027 (10 μM) on vacuolization in epidermoid cancer cells (A431) and immortal keratinocytes (HaCaT and Ker-CT) at 3, 6, and 12 h time points. Ker-CT or HaCaT exhibited significantly less pronounced cytoplasmic vacuolization compared with A431 cancer cells. (*D*) Histogram showing quantitative analyses of vacuolated cells. Between 4 and 6 randomly chosen fields with ∼100 cells/field for each treatment were evaluated for image analysis. This experiment represents 1 of 3 biological replicates. Cropped images presented here were captured at 100× (*A*) and 200× (*B* and *C*). ****$P < 0.0001$ compared with OSI-027–treated A431 cells.

These vacuoles were observed within 1 h of exposure and increased in size with time and finally merged with one another, creating giant cytoplasmic vacuoles, leading to eventual cytoplasmic membrane rapture and cell death (Fig. 2*B* and *SI Appendix*, Fig. S1*A*). Additional phenotypic changes as observed on phase-contrast microscopy of OSI-027–treated RD or RH30 cells include ruffling, contraction, and rounding (Fig. 2*B*). Transmission electron microscopy (TEM) confirmed the induction of massive vacuolization in OSI-027–treated RD cells (Fig. 2 *C*, *II* and *III*; compare with saline-treated control in *I*). Most of the large vesicles appeared empty and bounded by single membrane (Fig. 2 *C*, *III* and *III-b*, denoted by asterisks). Some surface membrane invaginations formed crater-like cups (Fig. 2 *C*, *III* and *III-a*, denoted by black arrows), and irregular surface membrane protrusions were also observed (*II*, denoted by red arrows). In contrast, ultrastructural differences were not observed in mitochondria (*SI Appendix*, Fig. S2*C*), endoplasmic reticulum (ER) (*SI Appendix*, Fig. S2*D*), or nuclear membrane morphology (*SI Appendix*, Fig. S2*E*) between control and OSI-027–treated RD cells at this treatment time point. These observations suggest that OSI-027–induced cell death occur mainly via an unconventional nonapoptotic mechanism.

OSI-027–Induced Cytoplasmic Vacuoles Are Macropinosomes. Rapid incorporation of extracellular-phase fluid tracer under projection of the plasma membrane during membrane ruffling is associated with the macropinosomes generation, a process known as macropinocytosis (1, 7). To investigate whether OSI-027– and PP242-induced vacuoles are macropinosomes, we incubated OSI-027–treated RMS cells with the tracer LY. LY in the medium was taken up by most of the cells within 1 h and increased within the cytoplasmic vacuoles in a time-dependent manner (Fig. 3*A* and *SI Appendix*, Fig. S3*A*). Most vacuoles within the cells were positive for LY and were macropinosomes (Fig. 3*A*). Internalization of LY was also observed in some saline-treated control cells, but the vacuoles were fewer in number and smaller in size compared with OSI-027–treated RMS cells (Fig. 3 *A* and *B*, *Left* and *SI Appendix*, Fig. S3*A*).

We further characterized the vacuoles for known macropinosome-specific markers (7, 26) by using indirect immunofluorescences staining with specific antibodies. OSI-027–induced vacuoles were positive for early endosome markers EEA1/Rab5 and late endosomal marker LAMP-1 (Fig. 3 *C* and *D* and *SI Appendix*, Fig. S3 *B* and *C*). In fact, OSI-027 significantly elevated most of these markers in RD cells and RH30 cells. It is well established that EEA1 and LAMP-1 can be detected in nonlysosomal compartments, such as early and late stages of endosomes (4, 19, 26). Bafilomycin A1 (BafA1), an inhibitor of the vacuolar-type H^+-ATPase, plays a crucial role in inhibiting vacuolization of late endosomes (27). OSI-027–induced cytoplasmic vacuolization in RD and RH30 cells was almost completely abrogated when the cells were pretreated with BafA1 (0.1 μM) for 1 h (Fig. 3 *E* and *F*). This BafA1-mediated inhibition of early- and late-phase macropinocytosis has been reported previously (28, 29).

Similar to RMS cells, OSI-027 treatment showed dose-dependent enhancement in immunofluorescence staining of LAMP-1 in HeLa, MCF7, and CW9019 cells (*SI Appendix*, Fig. S3 *D* and *E*). Superimposed bright field and fluorescence images confirmed the LY uptake in OSI-027–treated A431 cells, demonstrating the formation of macropinosomes (*SI Appendix*, Fig. S3*F*). These results clearly demonstrate that OSI-027 induces macropinocytosis in wide variety of cancer cells.

Dual Inhibition of mTORC1/2 Is Required for the Induction of Macropinocytosis. To confirm that OSI-027– and PP242-induced macropinocytosis is dependent on dual inhibition of mTORC1/2,

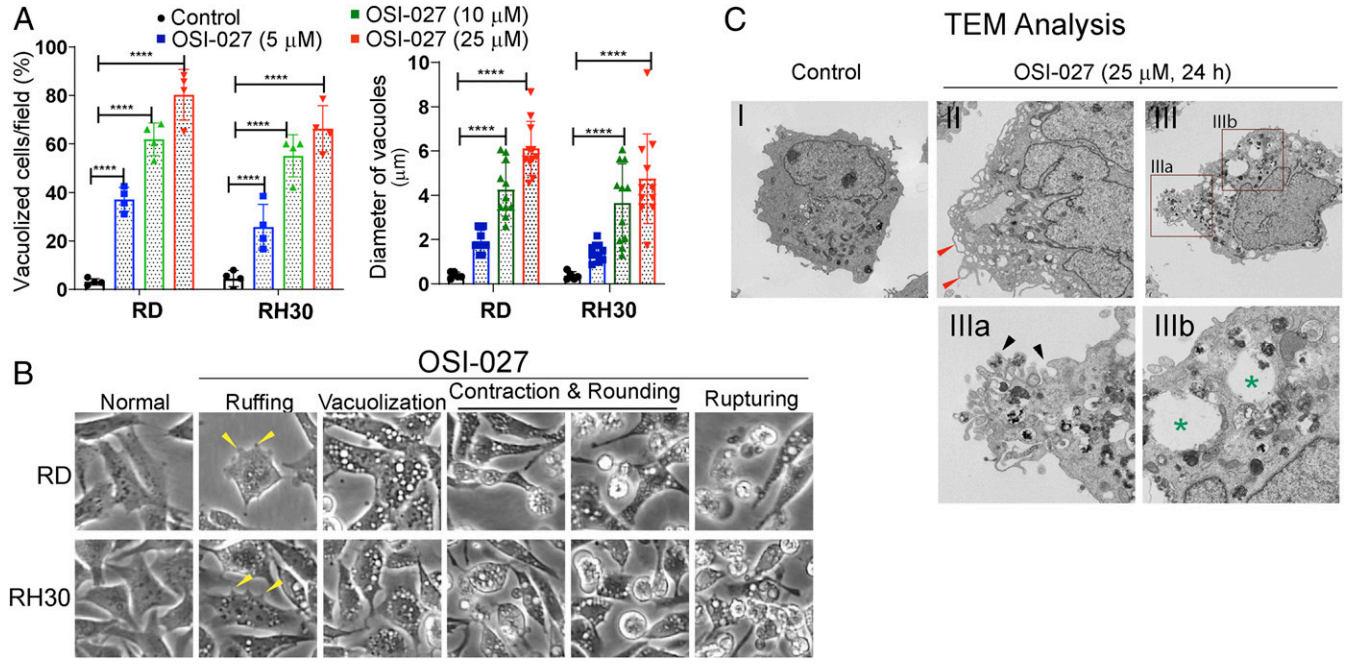

Fig. 2. OSI-027 induced dramatic phenotypic changes in RMS cells. (*A*) Concentration-dependent effects of OSI-027 (5 to 25 μM, 24 h) on the quantification (%) of vacuolized cells and average sizes of the vacuoles. Four or 5 different fields with 50 to 100 cells/field for each treatment were counted. ****$P < 0.0001$ compared with controls. This experiment is typical of 3 biological replicates. (*B*) Representative phase-contrast images showing ruffling (yellow arrows), vacuolization, contraction, rounding, and rupturing in OSI-027–treated RD or RH30 cells (see also *SI Appendix*, Fig. S1 *C*, and *Movie*). (Magnification: 100×.) (*C*) Representative TEM images of vehicle-treated (control) and OSI-027–treated (25 μM, 24 h) RD cells. *I*, control RD cells displaying well-maintained cytoplasmic compartments. *II* and *III*, OSI-027–treated cells showing massive vacuolization and degraded cytoplasmic compartments. In *II*, red arrows indicate the formation of plasma membrane-bound vacuoles and irregular protrusion compared with untreated plasma membrane cell surface. In *III*, *a*, black arrows indicate surface membrane invaginations formed crater-like cups. (Magnification: *C-I*, *II*, and *III*, 1,100×; *C-IIIa*, 2,100×; *C-IIIb*, 4,400×.) OSI-027–induced vacuoles varied in size and appeared mostly empty bound by single membrane (green asterisks in *III* and *III*, *b*).

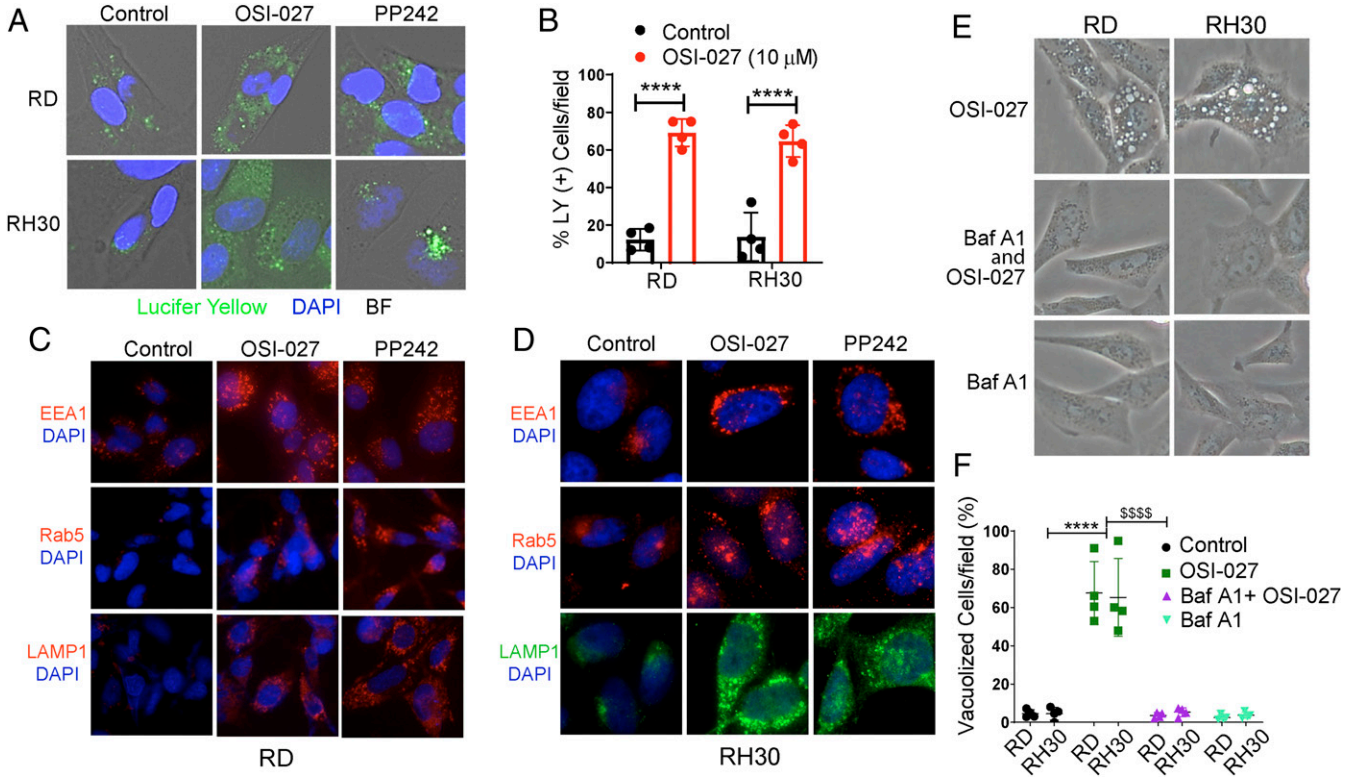

Fig. 3. Vacuoles induced by dual mTORC1/2 inhibitors are macropinosomes. (*A*) Overlay of bright field microphotographs on LY accumulation in untreated and OSI-027– or PP242-treated RD or RH30 cells at 24 h (also see *SI Appendix*, Fig. S3*A*). The majority of the vacuoles were positive for LY. The nature of the unstained vacuoles was not characterized. (*B*) Quantification of OSI-027–treated (10 μM, 24 h) LY-positive RD and RH30 cells compared with vehicle-treated control cells. (*C* and *D*) Fluorescence immunostaining for EEA1, Rab5, and LAMP-1 in RD (*C*) and RH30 (*D*) cells treated with vehicle (control), OSI-027 (10 μM, 24 h), or PP242 (2.5 μM, 24 h) (also see *SI Appendix*, Fig. S3 *C* and *D*). (*E* and *F*) Phase-contrast images (*E*) and bar graph (*F*) showing that BafA1 pretreatment (0.1 μM, 1 h) of RD and RH30 cells almost completely abrogated OSI-027–induced vacuolization. (Magnification: *A* and *D*, 400×; *C* and *E*, 200×.) $^{****}P < 0.0001$ compared with controls; $^{\$\$\$\$}P < 0.0001$ compared with OSI-027. Four to 5 fields of 50 to 100 cells/field for each treatment were counted. This experiment was repeated twice.

we performed siRNA knockdown of mTORC2 (Rictor) and then treated these cells with rapamycin, a widely known inhibitor of mTORC1 (30). Quantitative RT-PCR and immunoblot analyses confirmed the specific effects of Rictor siRNA knockdown and rapamycin treatment in RD cells (Fig. 4 *A* and *B*). Microscopically, Rictor siRNA in the presence or absence of rapamycin induced LY-containing vacuoles that were positive for LAMP-1 staining, similar to OSI-027–treated cells (Fig. 4*C*; compare columns 1, 2, 3, and 5), confirming the induction of macropinocytosis. In contrast, cells exposed to rapamycin alone did not significantly induce vacuoles; the cells exhibited a diffuse LY uptake and LAMP-1–positive vesicles were few and small (Fig. 4*C*, column 4). Quantitative analyses of single-agent and dual-agent treatment supported the visual interpretation (Fig. 4*D*). Furthermore, the average size of the vacuoles induced by the dual treatment was similar to that in OSI-027–treated cells, but with a lower percentage of cells with vacuoles (Fig. 4*D*). These data suggest that mTORC2 inhibition is important for macropinocytosis initiation and mTORC1 inhibition enhances this process.

We further confirmed some of these effects by using 2 additional dual mTORC1/2 inhibitors, MLN0128 (16) and Torin 1 (31). Both of these agents induced vacuolization in RD cells (Fig. 4*E*). Moreover, OSI-027, PP242, MLN0128, and Torin 1 treatment in RD cells reduced not only the phosphorylation of Raptor/Rictor, but also the downstream target proteins AKT, p70S6K, and 4EBP1 (Fig. 4*F*). Similar results were obtained in RH30 cells (*SI Appendix*, Fig. S4). We found a decrease in total Rictor and Raptor protein levels after treatment with these dual kinase inhibitors, similar to previously published data (32). The exact mechanism for this effect has not been determined; a possible explanation may be reduced protein stability because their ATP-binding pockets are occupied by these inhibitors.

MKK4 Is Involved in Macropinocytosis Induced by OSI-027 and PP242. We next investigated the possible involvement of other known signaling mechanisms that may contribute to the induction of macropinocytosis and eventual RMS cell death in OSI-027–treated cells. Based on previous reports, we focused mainly on defining the roles of pathways known to induce cell death caused by apoptosis (17), autophagy (23), or inappropriate expression of activated Ras/Rac1 (4).

Apoptosis is associated with a rapid loss of ATP and the activation of caspase 3. Treatment of RD and RH30 cells with OSI-027– or PP242-induced dose-dependent loss of cell viability (*SI Appendix*, Fig. S5 *A*, *I*). This observation was confirmed by ATP depletion in RD and RH30 cells on OSI-027 treatment in a time-dependent manner (*SI Appendix*, Fig. S5 *A*, *II*). However, active cleaved caspase-3 did not show significant induction when probed with immunofluorescence and for enzymatic activity (Fig. 5*A* and *SI Appendix*, Fig. S5*B*). As a positive control for cleaved caspase-3, we treated cells with arsenic trioxide, a known inducer of apoptotic cell death (33). We detected significant increase in the cleaved caspase-3 protein and enzymatic activity (Fig. 5*A* and *SI Appendix*, Fig. S5*B*). These results suggest that OSI-027– and PP242-induced cell death is mediated largely by a nonapoptotic mechanism.

Autophagy-associated cell death is the most widely studied form of nonapoptotic cell death and has been attributed to mTOR inhibition (34). However, our immunofluorescence staining and immunoblotting showed that autophagy biomarker proteins LC3A/B,

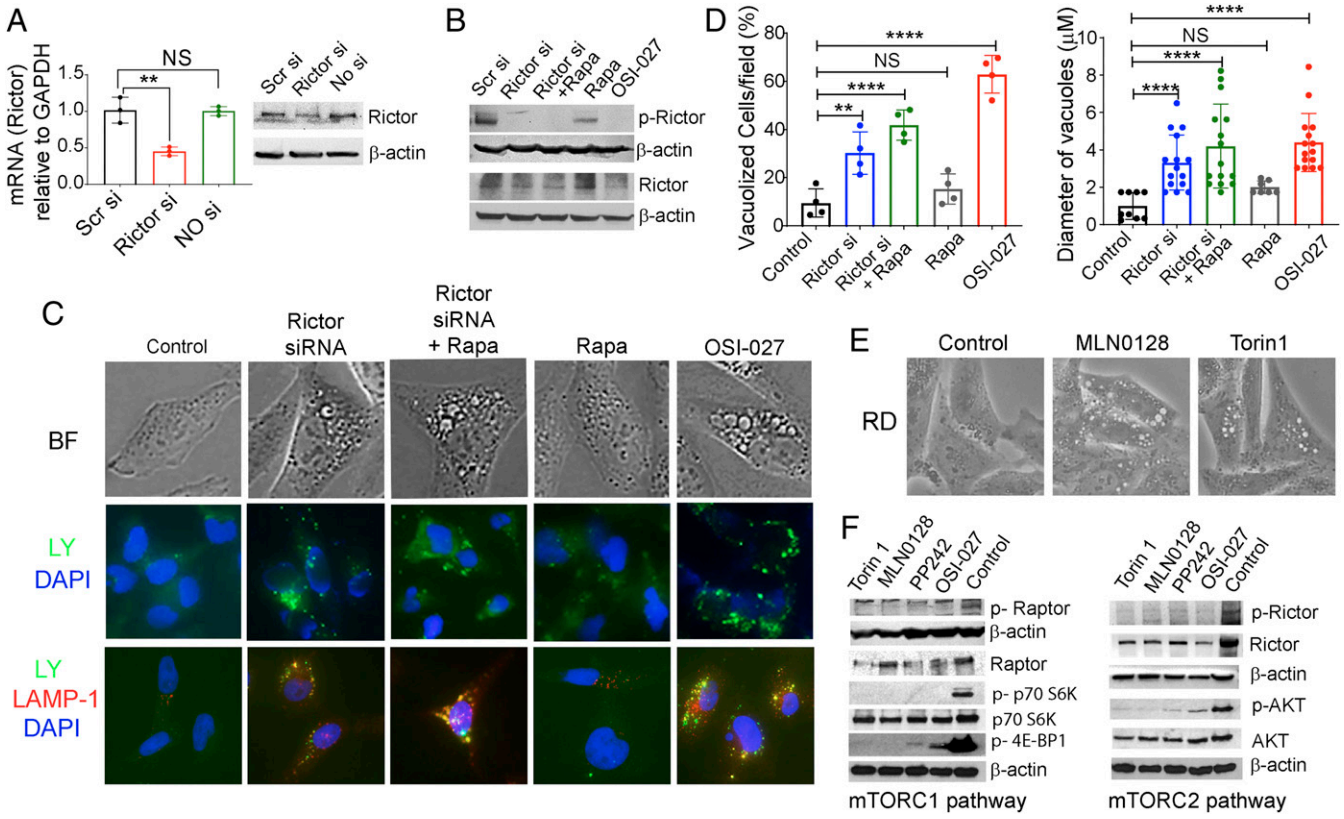

Fig. 4. mTORC2 has a more important role than mTORC1 in controlling macropinocytosis. (*A*) Real-time RT-PCR mRNA analyses and protein immunoblots showing the efficiency of knockdown of Rictor expression in RD cells. A scramble siRNA (Scr si) or no siRNA served as a negative control. β-actin served as a protein loading control. (*B*) Immunoblot analyses of p-Rictor/Rictor in the presence or absence of siRNAs, rapamycin, or OSI-027 in RD cells. (*C*) Bright field (BF) micrographs (*Upper*), LY yellow uptakes (*Middle*) and dual immunofluorescence staining of LAMP-1 with LY-positive RD cells (*Lower*) in the presence or absence of indicated treatments. Cropped images presented here were captured at 400× (*Upper* and *Lower*) and 200× (*Middle*). (*D*) Quantification of vacuolized cells and average vacuole sizes in the presence or absence of the indicated treatments. Four to 5 fields with ∼50 cells/field for each treatment were counted. $^{**}P < 0.01$; $^{****}P < 0.0001$ compared with controls. NS, not significant compared with controls. (*E*) Photomicrograph showing vacuolization in RD cells induced by MLN0128 (2.5 μM, 24 h) and Torin 1 (1 μM, 24 h). (Magnification: 400×.) (*F*) Immunoblot analyses of mTORC1 and mTORC2 signaling proteins in RD cell lysates treated with mTORC1/2 inhibitors (OSI-027, 10 μM; PP242, 2.5 μM; MLN0128, 2.5 μM; Torin 1, 1 μM) for 24 h. The experiments shown here were repeated twice.

ATG7, and Beclin-1 were not induced in the RMS cells treated with OSI-027 (Fig. 5*B* and *SI Appendix*, Fig. S6 *A* and *B*). In contrast, the positive controls generated by treatment of RD cells with rapamycin (0.5 μM, 24 h), a known inducer of autophagy, significantly elevated the expression of LC-3A/B (Fig. 5*B*). Similarly, rapamycin-treated, but not OSI-027-treated, RMS cells showed appreciable staining with dansylcadaverine (*SI Appendix*, Fig. S6*C*), an autofluorescent dye used to monitor autophagy (35). It is interesting to note that dual inhibition of mTORC1 and mTORC2 induces macropinocytosis but has little effect on autophagy, whereas mTORC1 inhibition largely induces widespread autophagy, as reported previously (34).

Ras signaling was shown to underlie macropinocytosis in glioblastoma cells (4). Rac1, a downstream signal molecule of Ras, is required to induce these lethal vacuoles (36). Interestingly, in RMS cells, OSI-027 significantly increased the phosphorylation of Rac1 as assessed by indirect immunofluorescence (*SI Appendix*, Fig. S7*A*) and immunoblotting (Fig. 5*C*). However, blockade of Rac1 signaling by using its specific inhibitor NSC23766 (37) or Rac1 siRNA did not rescue these cells from massive vacuolization (Fig. 5*D* and *SI Appendix*, Fig. S7 *B–D*). These data are inconsistent with a significant role of Rac1 in the induction of macropinocytosis by the dual mTORC1/2 inhibitors in RMS cells.

Recent studies also have discussed the involvement of MAP kinase MKK4 as a key signaling molecule in invoking macropinocytosis (3, 38). We indeed detected activation of MKK4 phosphorylation by the dual mTORC1/2 inhibitors in RMS cells (Fig. 5*E*). Importantly, MKK4 (denoted by the *MAP2K4* gene) silencing by siRNA (*SI Appendix*, Fig. S8*A*) abolished cell phenotypic changes related to macropinosomes generation (Fig. 5*F*). This observation was confirmed by a reduced percentage of vacuolized RD cells upon knockdown (Fig. 5*G* and *SI Appendix*, Fig. S8*B*).

We next investigated the mechanism by which the dual mTOR kinase inhibitors activate MKK4. MKK4 kinase is redox-sensitive and is induced by ROS production (39). Indeed, we found that OSI-027 augmented ROS production in RD cells (Fig. 5*H*). To test the hypothesis that ROS generated by OSI-027 activate MKK4, we treated RD cells with the antioxidant *N*-acetyl-L-cysteine (NAC) before exposure to the mTORC1/2 inhibitor. NAC treatment reduced both OSI-027–induced ROS production and MKK4 phosphorylation (Fig. 5 *H* and *I*). Vacuole formation was also diminished (Fig. 5*J*).

OSI-027 Blocks Human RMS Cell-Derived Xenograft Tumor Growth by Inducing Macropinocytosis. To complement our in vitro studies, we further investigated whether OSI-027–mediated macropinocytosis could contribute to curbing RMS tumor growth in the murine xenograft model. Following inoculation of RD and RH30 cells in nude mice, groups of 5 mice each were randomized into control and experimental groups. Starting at 1 d postimplantation, control mice received only an oral gavage of vehicle until the mice had to be killed owing to the large tumor sizes at 33 d for mice xenografted

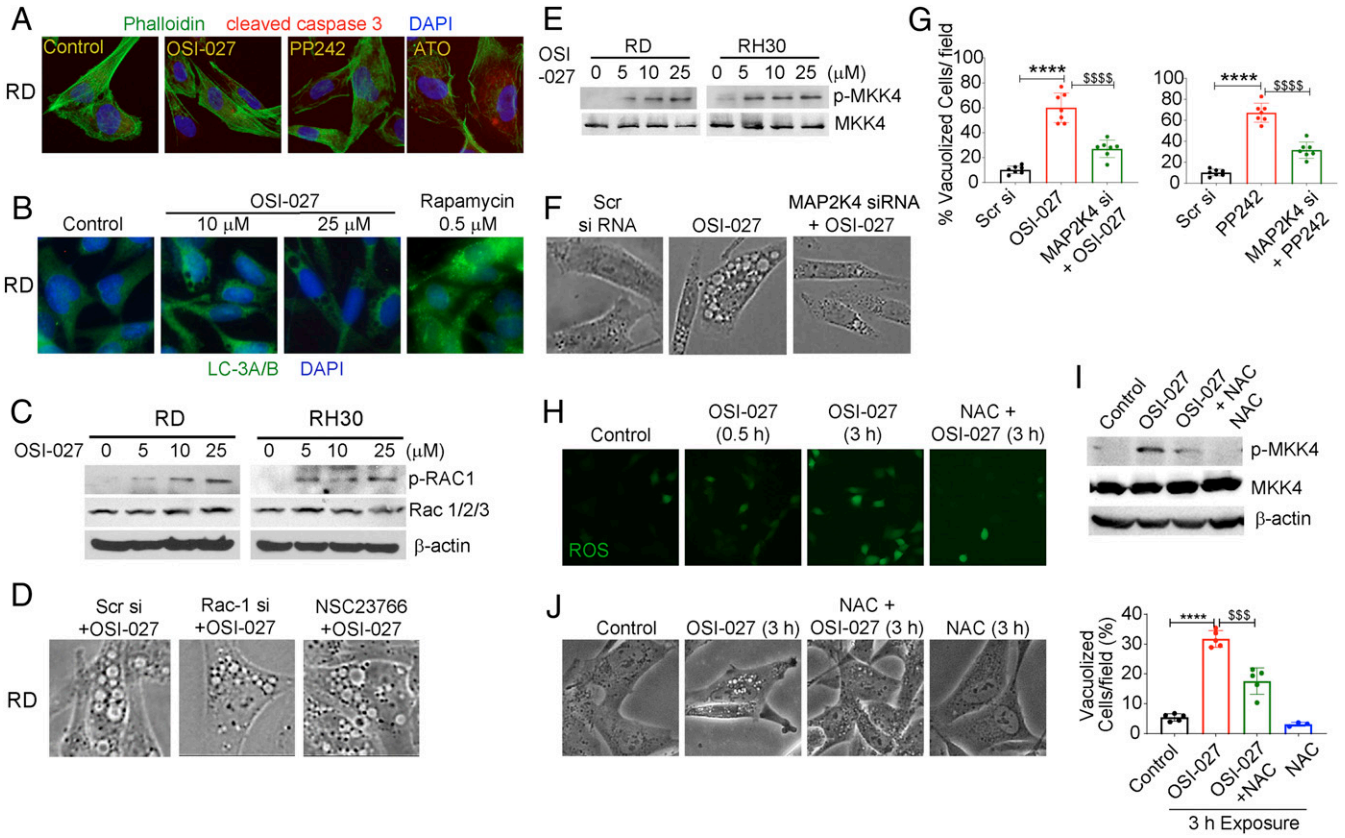

Fig. 5. MKK4 is involved in macropinocytosis induction in RMS cells. (*A*) Active cleaved caspase-3 (red) and phalloidin counterstaining (green) in RD cells treated with OSI-027 (10 μM, 24 h), PP242 (2.5 μM, 24 h), and arsenic trioxide (ATO) (4 μM, 24 h). (*B*) Immunofluorescence staining of LC3A/B in vehicle-treated (control) or OSI-027–treated (10 and 25 μM, 24 h) RD cells. Rapamycin (Rapa) (0.5 μM, 24 h) served as a positive control as an autophagy marker. (*C*) Immunoblot analyses of p-Rac1 and Rac1/2/3 proteins in OSI-027–treated RD and RH30 cells. (*D*) Phase-contrast images showing that reduction or inhibition of Rac1 by Rac1 siRNA and NSC23766, a specific inhibitor for Rac1, did not protect RD cells from OSI-027–induced vacuolization. (*E*) Immunoblots of p-MKK4 and MKK4 in OSI-027–treated RD and RH30 cells. (*F*) Phase-contrast images showing that knockdown of MKK4 by MAP2K4 siRNA significantly reduced OSI-027–induced vacuolization in RD cells. Scr siRNA served as a negative control. (*G*) Quantification of vacuolized cells in MKK4 knockdown RD cells treated with OSI-027 or PP242. ****$P < 0.0001$ compared with Scr si; $^{\$\$\$\$}P < 0.0001$ compared with OSI-027 or PP242. (*H*) ROS detected by green fluorescence of the DCF-DA probe in RD cells treated with OSI-027 (10 μM, 3 h) in the presence and absence of NAC (5 mM). (*I*) Immunoblot analysis of p-MKK4 and MKK4 in RD cell lysates treated with OSI-027 (10 μM, 3 h) in the presence and absence of NAC. (*J*) Phase-contrast images of RD cells following treatment with OSI-027 (10 μM, 3 h) in the presence and absence of NAC. The histogram shows the percentages of vacuolized cells. Cropped images presented here were captured at 200× (*A*, *B*, *F*, and *J*) or 400× (*D*), while *H* captured at 400× but not cropped. ****$P < 0.0001$ compared with controls; $^{\$\$\$}P < 0.001$ compared with OSI-027.

with RD cells and at 21 d for mice xenografted with RH30 cells. The experimental group received OSI-027 (150 mg/kg 3 times per wk) and were killed at the same time. At the end of the experiment, the OSI-027-treated mice showed a 90% reduction in RD cell-derived tumor growth and a 61% reduction of RH30 cell-derived tumor growth (Fig. 6*A*). Thus, the 2 RMS cell lines exhibited differing tumor growth rates and sensitivities to OSI-027.

The histology of these hematoxylin and eosin-stained tumor sections showed prominent vacuolated cells in only OSI-027–treated residual RD and RH30 xenograft tumors (Fig. 6*B*, denoted by black arrows). Furthermore, the residual tumor tissues showed elevated LAMP-1 and EEA1 proteins (Fig. 6 *C* and *D*). These observations are consistent with the interpretation that OSI-027–mediated tumor inhibition is attributable to macropinocytosis, an unconventional nonapoptotic mechanism. However, unlike our in vitro results, we detected a slight increase in TUNEL and cleaved caspase-3–positive cells in OSI-027–treated RH30 residual tumors (*SI Appendix*, Fig. S9 *A* and *B*). These results suggest that a level of apoptosis was also induced, helping curb tumor growth.

By immunofluorescence staining, we also confirmed that residual tumors of OSI-027–treated animals manifested reduced p-AKT/p-mTOR (*SI Appendix*, Fig. S9*C*) and cell proliferation marker proteins Cyclin D1 and PCNA (*SI Appendix*, Fig. S9*D*). In cultured RD and RH30 cells, OSI-027 exposure also reduced cyclin D1 expression (*SI Appendix*, Fig. S10*A*), as well as colony formation by RD cells (*SI Appendix*, Fig. S10*B*).

OSI-027 Treatment Synergistically Enhances the Efficacy of Cyclophosphamide Against Established RMS Derived Xenograft Tumors. Cyclophosphamide is a standard care treatment for RMS in pediatric patients (40, 41). Therefore, we tested whether blocking mTORC1/2 by OSI-027 could enhance the efficacy of cyclophosphamide in a preestablished RMS-derived xenograft tumor model. Animals receiving each cell type were randomized into control and experimental groups ($n = 5$ in each group). Treatment was initiated when the animals developed tumors ~80 mm^3 in size. 75 mg/kg OSI-027 (in corn oil, orally, 3 times/wk) or 60 mg/kg cyclophosphamide (in PBS, intraperitoneal, 2 times/wk) were administered alone or in combination for up to 49 d. We did not observe any significant changes in mouse body weight during the course of drug treatment (*SI Appendix*, Fig. S11*A*). The abilities of the agents to reduce the growth of RMS cell xenograft tumors were comparable and significant, more so in RD (eRMS subtype) tumors compared with RH30 (aRMS subtype) tumors (Fig. 7 *A*, *B*, *D*, and *E*). Importantly, the combination treatment was much more effective than the single treatments. The growth of RH30

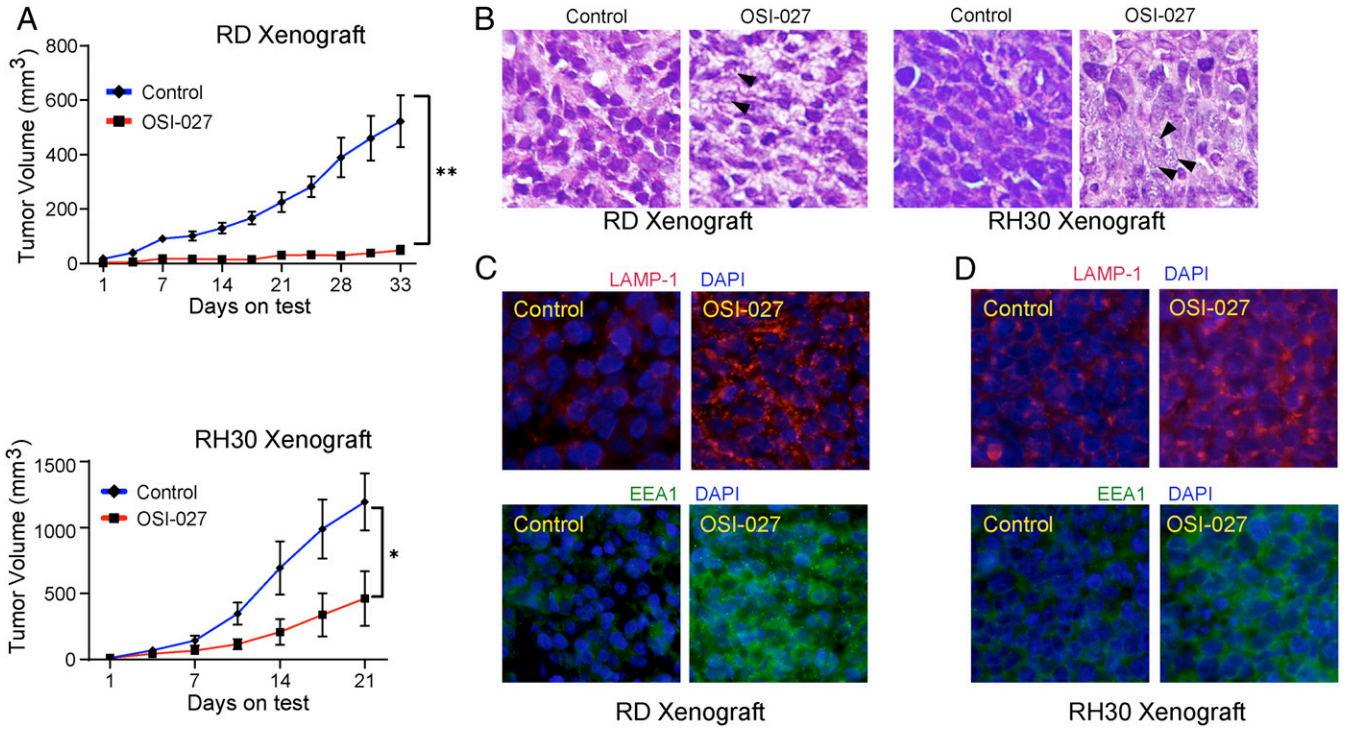

Fig. 6. OSI-027 reduces human RMS cell-derived xenograft tumor growth by inducing macropinocytosis. (*A*) Line graph showing the inhibitory effects of OSI-027 (150 mg/kg orally, 3 times/wk, starting at 1 d after tumor cell grafting) on the tumor volume of RD and RH30 cell-derived xenograft tumors ($n = 5$/group). *$P < 0.05$; **$P < 0.01$ compared with vehicle-treated controls. (*B*) Hematoxylin and eosin staining of the 5-μm sections of tumors derived from xenografted RD cells (*Left*) and RH30 cells (*Right*) harvested on day 33 and day 21, respectively. Arrowheads denote vacuolated and ruptured cells. (*C* and *D*) Immunofluorescence staining of LAMP-1 and EEA1 in the tumor sections of vehicle- or OSI-027–treated RD (*C*) and RH30 (*D*) cell-derived xenografts. (Magnification: *A*, *C*, and *D*, 400×.) Photographs were captured using an Olympus BX51 microscope.

xenograft tumors was static following the dual treatment. The residual tumors showed highly necrotic areas in hematoxylin and eosin-stained sections (Fig. 7*C* and *SI Appendix*, Fig. S11*B*). In contrast, the RD xenograft tumors showed regression (Fig. 7 *D* and *E*). The residual tumors were highly vacuolated and mostly enucleated (Fig. 7*F* and *SI Appendix*, Fig. S11*C*).

OSI-027 Treatment Inhibits Epithelial Mesenchymal Transition of Human RMS Cell-Derived Xenograft Tumors. mTORC1 and mTORC2 components of the mTOR signaling pathways have been shown to regulate epithelial mesenchymal transition (EMT) in colorectal cancer (42). We have also reported that in RMS-derived xenograft tumors, the combined Sonic Hedgehog and AKT-mTOR signaling pathways regulate EMT (13, 14). We thus tested whether the inhibitor of the mTOR complexes would also modulate the expression of proteins that regulate EMT. Immunofluorescence analyses showed that in OSI-027–treated RD or RH30 cell-derived xenografts, the epithelial biomarker E-cadherin was increased, whereas mesenchymal biomarkers fibronectin and vimentin were decreased (Fig. 8 *A* and *C*). Immunofluorescence and immunoblot assays conducted on residual tumors also showed that the transcription factors that promote EMT, such as Snail, Twist, and Slug, were reduced in OSI-027–treated animals compared with vehicle-treated animals (Fig. 8 *A*–*D*).

Discussion

mTOR pathway is the key signaling mechanism that integrates multiple intracellular and extracellular cues, ultimately regulating multiple complex cellular processes including cell metabolism, proliferation, angiogenesis, and survival (8, 43). Thus, both mTORC1 and mTORC2 play key roles in the pathogenesis of tumor growth in multiple organs (44). Many neoplasms that are driven by impairment in tumor suppressor mechanisms or activation of oncogenic signaling have been documented to have augmented serine/threonine kinases in the mTORC1/mTORC2 pathways (45, 46). mTORC1 has been studied in great detail, whereas mTORC2 has been investigated less extensively. mTORC2 is activated by growth factors (47, 48) and has been considered important for the maximum activation of AKT by phosphorylating it at serine 473 (49). In addition, it activates other kinases, such as S6K and protein kinase C (PKC) family members, thereby contributing to the pathogenesis of tumors (50). Although it is likely that blockade of upstream regulating oncogenic pathways may dampen this downstream tumor-promoting mTORC1/mTORC2 signaling, tumors often become nonresponsive due to the resurgent downstream mTOR complexes. Indeed, mTORC1 inhibitors rapamycin and other rapalogs initially showed some promise in treating cancers, but their chronic administration resulted in drug resistance due to feedback activation of AKT/PI3K pathways by mTORC2 (15, 51). Therefore, simultaneous blocking of downstream mTORC1/2 signaling would enhance the efficacy of drugs blocking the upstream tumor-initiating pathways (16, 52, 53).

Here we identified that dual inhibitors of mTORC1/mTORC2, such as OSI-027, PP242, MLN0128, and Torin 1, are potent inducers of macropinocytosis, a distinct but rarely described form of cell death (1). Previously, specific inducers of macropinocytosis, such as Vacquinol-1, MOPIPP, silmitasertib, and tubeimoside-1, were found to manifest this response mainly in glioblastomas and colorectal cells (3, 38, 54, 55). In contrast, our study demonstrates that these dual inhibitors induce catastrophic vacuolization in tumor cell lines from a wide range of organs, including skin, breast, cervical, lung, and soft tissues. Based on LY uptake, it is clear that the majority of these induced vacuoles are macropinosomes. Moreover, our findings demonstrate a critical role of mTORC2 in

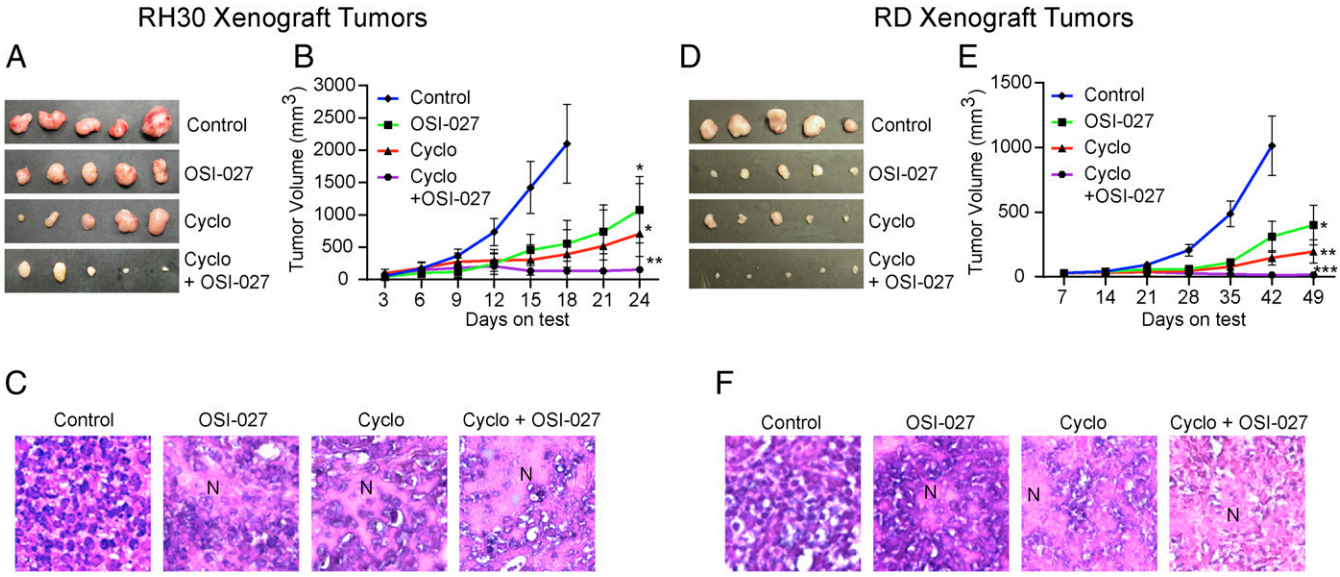

Fig. 7. OSI-027 enhances the inhibitory efficacy of cyclophosphamide against RMS cell-derived xenograft tumors. Tumors were derived from RH30 cells (*A*–*C*) or RD cells (*D*–*F*). Tumor volumes were ~80 mm^3 when treatments started. (*A* and *D*) Representative tumors excised from vehicle- or drug-treated animals ($n = 5$). (*B* and *E*) Line graphs showing the inhibitory effects of OSI-027 (75 mg/kg orally, 3 times/wk), cyclophosphamide (Cyclo) (60 mg/kg, i.p., 2 times/wk), or both on the growth of xenograft tumors. (*C* and *F*) Hematoxylin and eosin staining of the 5-μm sections of formalin-fixed xenograft tumors. (Magnification: *A*, 100×; *B* and *C*, 200×.) Tumor sections from vehicle-treated control animals show highly condensed areas of proliferating cells with dark nuclei, whereas the sections from OSI-027–treated and/or cyclophosphamide-treated animals show disrupted tumor tissue architecture associated with necrotic patches (N). $*P < 0.05$; $**P < 0.01$; $***P < 0.001$ compared with vehicle-treated control tumors. Each set of data represents $n = 5$.

suppressing macropinocytosis, as knockdown of mTORC2 (Rictor) alone can induce macropinocytosis in RMS cells. This response is further augmented by inhibiting mTORC1 with rapamycin, a classic mTORC1 inhibitor (Fig. 4). Interestingly, mTORC2 also suppressed autophagy caused by inhibition of mTORC1 (Fig. 5*B* and *SI Appendix*, Fig. S6*B*).

Our xenograft data in athymic mice show that the dual mTORC1/mTORC2 inhibitors significantly reduced RMS tumor growth, primarily via macropinocytosis as in vitro. These inhibitors were much more effective when administered along with cyclophosphamide, a chemotherapeutic agent used as standard treatment for patients with a variety of cancers (Figs. 6 and 7). Furthermore, the dual mTOR inhibitors not only inhibited growth, but also altered tumor properties. The residual tumors showed strong epithelial phenotypes. In particular, the epithelial marker E-cadherin was up-regulated, whereas the mesenchymal markers Vimentin, Snail, Slug, and Twist were significantly down-regulated (Fig. 8). This is in line with the reported impact of mTORC2 on multiple pathways (42, 56, 57). For instance, mTORC2 directly interacts with ribosomes by promoting the phosphorylation of AKT (T450) at turn motif sites and of several PKCs, ultimately leading to cell survival. In addition, it affects cancer cell chemotaxis by activating actin polymerization and metastasis (58). The inhibition of mTORC2 would then lead to less aggressive tumors,

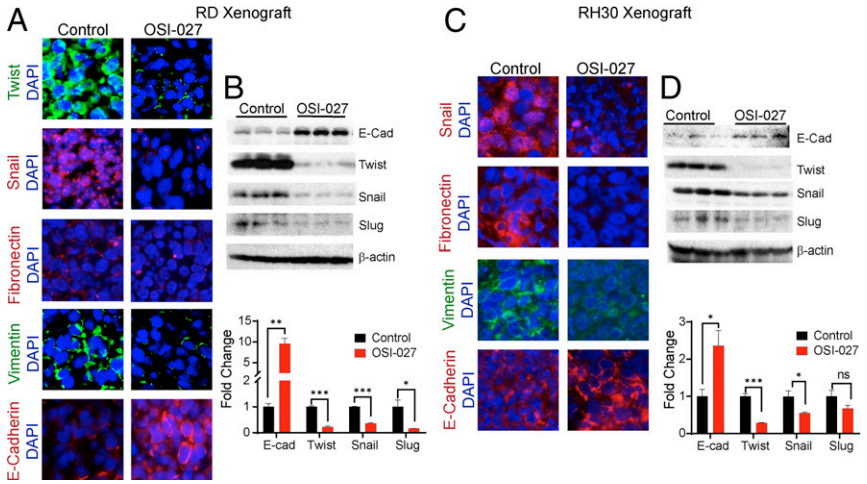

Fig. 8. OSI-027 down-regulates the expression of biomarkers of EMT in RMS xenograft tumors. (*A* and *C*) Immunofluorescence staining of Twist, Snail, Fibronectin, Vimentin, and E-cadherin (E-cad) in vehicle- or OSI-027–treated RMS cell-derived xenograft tumors harvested on day 33 for RD or on day 21 for RH30. (Magnification: 400×.) (*B* and *D*) Immunoblot analysis of E-cadherin (E-Cad), Twist, Snail, and Slug in tumor lysates obtained from vehicle- and OSI-027–treated animals on termination of the experiment. The histogram shows a densitometry analysis of immunoblot band intensity. $*P < 0.05$; $**P < 0.01$; $***P < 0.001$ compared with their respective controls. ns, nonsignificant. Each set of data represents $n = 3$.

as also observed in our study (Fig. 8). Here we also observed some differences in the response of mTORC1/mTORC2 dual inhibitors in abrogating tumor growth of eRMS and aRMS representing RD and RH30 cell-derived xenografts. These differences could be due to the cross-talk of tumor-specific tumor driver pathways with mTOR signaling. Further studies are needed to delineate these differential responses.

Ras/Rac1 signaling has previously been implicated in regulating cell death by macropinocytosis (4, 59). However, we could not confirm any role of this signaling pathway in mTORC2-dependent macropinocytosis (Fig. 5*D*). It is possible that the Ras/Rac1 pathway has overlapping roles in a cell context-dependent manner. Rather, our findings demonstrate that the molecular mechanism underpinning mTORC2-regulated macropinocytosis involves the activation of MKK4, as its blockade abrogates this response (Fig. 5). The mechanism by which MKK4 participates in the development of macropinosomes is not well understood but likely involves membrane ruffling and closure of macropinosomes. However, unlike in an earlier report (60), here we found that the PI3K/AKT signaling pathway is not a likely contributor, as AKT phosphorylation is diminished by the dual inhibitor (Fig. 4*F*). Nevertheless, we demonstrate a role of ROS in phosphorylation-dependent activation of MKK4 and its subsequent involvement in macropinocytosis (Fig. 5). Recently, Wnt signaling was shown to play some role in the intake of large amounts of extracellular fluid by macropinosomes (61). Additional studies are needed to pinpoint exactly how mTORC2 connects MAP kinase and other signaling pathways to macropinocytosis.

In summary, our data reveal that therapeutic targeting of mTORC1 and mTORC2 together with standard care treatment may be an effective approach to block the pathogenesis of recurrent RMS and perhaps other drug-resistant invasive neoplasms of diverse tissue types as well. The underlying mechanism by which tumors become responsive to treatment involve macropinocytosis, a unique form of cell death.

Materials and Methods

Human RMS cells RH30 and RD, human epidermoid carcinoma cell line A431, human breast adenocarcinoma cell line MCF7, human lung adenocarcinoma epithelial cell line A549, human cervical cancer cell line HeLa, and the human immortalized foreskin keratinocytes (Ker-CT) were procured from American Type Culture Collection. The immortalized human keratinocyte cell line HaCaT was obtained from AddexBio. Two other human RMS cell lines corresponding to eRMS (SMS-CTR) and aRMS (CW9019) were provided by Frederic G. Barr of the National Cancer Institute. OSI-027, MLN0128, and Torin 1 were purchased from Selleckchem. Rapamycin was obtained from LC Laboratories. Cyclophosphamide monohydrate, BafA1, *N*-acetyl-L-cysteine, and PP242 were purchased from Sigma-Aldrich. NSC23766 was obtained from Santa Cruz Biotechnology. siRNAs against human MAP2K4, Rac1, and Rictor were procured from Life Technology. 2′,7′-Dichlorofluorescein diacetate probe and dextran LY and Phalloidin dye were purchased from Invitrogen. Dansylcadaverine dye was obtained from Sigma-Aldrich. Treatments of various cells in culture were performed at confluency of ∼70%.

All animal procedures were performed according to guidelines of and under approval from the Institutional Animal Care and Use Committee of the University of Alabama at Birmingham. Additional information on materials, experimental protocols, and statistical analyses are provided in *SI Appendix*.

Data Availability. All additional data and information are included in the *SI Appendix* as figures, additional materials, methods, references, and tables for antibodies, sources, uses, and dilutions.

ACKNOWLEDGMENTS. This work was supported by NIH Grant R01 ES026219 (to M.A.). M.A. is also supported by an Eric Baum Endowed Professorship. N.S.B. and L.T.C. are supported by funds from the Anderson Family Endowed Chair through the University of Alabama at Birmingham.

1. W. A. Maltese, J. H. Overmeyer, Non-apoptotic cell death associated with perturbations of macropinocytosis. *Front. Physiol.* **6**, 38 (2015).
2. D. Tang, R. Kang, T. V. Berghe, P. Vandenabeele, G. Kroemer, The molecular machinery of regulated cell death. *Cell Res.* **29**, 347–364 (2019).
3. E. Silva-Pavez *et al*., CK2 inhibition with silmitasertib promotes methuosis-like cell death associated to catastrophic massive vacuolization of colorectal cancer cells. *Cell Death Dis.* **10**, 73 (2019).
4. J. H. Overmeyer, A. Kaul, E. E. Johnson, W. A. Maltese, Active ras triggers death in glioblastoma cells through hyperstimulation of macropinocytosis. *Mol. Cancer Res.* **6**, 965–977 (2008).
5. C. Li *et al*., Unravelling the mechanism of TrkA-induced cell death by macropinocytosis in medulloblastoma daoy cells. *Mol. Cell. Biol.* **36**, 2596–2611 (2016).
6. M. Colin *et al*., Dysregulation of macropinocytosis processes in glioblastomas may be exploited to increase intracellular anti-cancer drug levels: The example of temozolomide. *Cancers (Basel)* **11**, E411 (2019).
7. J. A. Swanson, C. Watts, Macropinocytosis. *Trends Cell Biol.* **5**, 424–428 (1995).
8. R. A. Saxton, D. M. Sabatini, mTOR signaling in growth, metabolism, and disease. *Cell* **168**, 960–976 (2017).
9. M. Laplante, D. M. Sabatini, mTOR signaling at a glance. *J. Cell Sci.* **122**, 3589–3594 (2009).
10. H. Pópulo, J. M. Lopes, P. Soares, The mTOR signalling pathway in human cancer. *Int. J. Mol. Sci.* **13**, 1886–1918 (2012).
11. A. L. Kim *et al*., SOX9 transcriptionally regulates mTOR-induced proliferation of basal cell carcinomas. *J. Invest. Dermatol.* **138**, 1716–1725 (2018).
12. P. B. Crino, The mTOR signalling cascade: Paving new roads to cure neurological disease. *Nat. Rev. Neurol.* **12**, 379–392 (2016).
13. R. K. Srivastava *et al*., GLI inhibitor GANT-61 diminishes embryonal and alveolar rhabdomyosarcoma growth by inhibiting the Shh/AKT-mTOR axis. *Oncotarget* **5**, 12151–12165 (2014).
14. S. Z. Kaylani *et al*., Rapamycin targeting mTOR and hedgehog signaling pathways blocks human rhabdomyosarcoma growth in xenograft murine model. *Biochem. Biophys. Res. Commun.* **435**, 557–561 (2013).
15. K. E. O'Reilly *et al*., mTOR inhibition induces upstream receptor tyrosine kinase signaling and activates Akt. *Cancer Res.* **66**, 1500–1508 (2006).
16. E. K. Slotkin *et al*., MLN0128, an ATP-competitive mTOR kinase inhibitor with potent in vitro and in vivo antitumor activity, as potential therapy for bone and soft-tissue sarcoma. *Mol. Cancer Ther.* **14**, 395–406 (2015).
17. S. V. Bhagwat *et al*., Preclinical characterization of OSI-027, a potent and selective inhibitor of mTORC1 and mTORC2: Distinct from rapamycin. *Mol. Cancer Ther.* **10**, 1394–1406 (2011).
18. Y. Zheng, Y. Jiang, mTOR inhibitors at a glance. *Mol. Cell. Pharmacol.* **7**, 15–20 (2015).
19. N. R. Cook, P. E. Row, H. W. Davidson, Lysosome-associated membrane protein 1 (Lamp1) traffics directly from the TGN to early endosomes. *Traffic* **5**, 685–699 (2004).
20. F. T. Mu *et al*., EEA1, an early endosome-associated protein. EEA1 is a conserved alpha-helical peripheral membrane protein flanked by cysteine "fingers" and contains a calmodulin-binding IQ motif. *J. Biol. Chem.* **270**, 13503–13511 (1995).
21. C. Mecca *et al*., PP242 counteracts glioblastoma cell proliferation, migration, invasiveness and stemness properties by inhibiting mTORC2/AKT. *Front. Cell. Neurosci.* **12**, 99 (2018).
22. B. W. Chen *et al*., Inhibition of mTORC2 induces cell-cycle arrest and enhances the cytotoxicity of doxorubicin by suppressing MDR1 expression in HCC cells. *Mol. Cancer Ther.* **14**, 1805–1815 (2015).
23. H. O. Jin *et al*., Inhibition of JNK-mediated autophagy enhances NSCLC cell sensitivity to mTORC1/2 inhibitors. *Sci. Rep.* **6**, 28945 (2016).
24. B. Blaser *et al*., Antitumor activities of ATP-competitive inhibitors of mTOR in colon cancer cells. *BMC Cancer* **12**, 86 (2012).
25. F. Musa *et al*., Dual mTORC1/2 inhibition as a novel strategy for the resensitization and treatment of platinum-resistant ovarian cancer. *Mol. Cancer Ther.* **15**, 1557–1567 (2016).
26. M. Hamasaki, N. Araki, T. Hatae, Association of early endosomal autoantigen 1 with macropinocytosis in EGF-stimulated A431 cells. *Anat. Rec. A Discov. Mol. Cell. Evol. Biol.* **277**, 298–306 (2004).
27. T. Yoshimori, A. Yamamoto, Y. Moriyama, M. Futai, Y. Tashiro, Bafilomycin A1, a specific inhibitor of vacuolar-type H(+)-ATPase, inhibits acidification and protein degradation in lysosomes of cultured cells. *J. Biol. Chem.* **266**, 17707–17712 (1991).
28. M. V. Recouvreux, C. Commisso, Macropinocytosis: A metabolic adaptation to nutrient stress in cancer. *Front. Endocrinol. (Lausanne)* **8**, 261 (2017).
29. S. Kitazawa *et al*., Cancer with low cathepsin D levels is susceptible to vacuolar (H^+)-ATPase inhibition. *Cancer Sci.* **108**, 1185–1193 (2017).
30. M. Athar, L. Kopelovich, Rapamycin and mTORC1 inhibition in the mouse: Skin cancer prevention. *Cancer Prev. Res. (Phila.)* **4**, 957–961 (2011).
31. C. C. Thoreen *et al*., An ATP-competitive mammalian target of rapamycin inhibitor reveals rapamycin-resistant functions of mTORC1. *J. Biol. Chem.* **284**, 8023–8032 (2009).
32. S. Xu *et al*., Impact on autophagy and ultraviolet B-induced responses of treatment with the MTOR inhibitors rapamycin, everolimus, torin 1, and pp242 in human keratinocytes. *Oxid. Med. Cell. Longev.* **2017**, 5930639 (2017).
33. R. Mahieux *et al*., Arsenic trioxide induces apoptosis in human T-cell leukemia virus type 1- and type 2-infected cells by a caspase-3-dependent mechanism involving Bcl-2 cleavage. *Blood* **98**, 3762–3769 (2001).
34. Y. C. Kim, K. L. Guan, mTOR: A pharmacologic target for autophagy regulation. *J. Clin. Invest.* **125**, 25–32 (2015).
35. A. Biederbick, H. F. Kern, H. P. Elsässer, Monodansylcadaverine (MDC) is a specific in vivo marker for autophagic vacuoles. *Eur. J. Cell Biol.* **66**, 3–14 (1995).

36. M. Fujii, K. Kawai, Y. Egami, N. Araki, Dissecting the roles of Rac1 activation and deactivation in macropinocytosis using microscopic photo-manipulation. *Sci. Rep.* **3**, 2385 (2013).
37. Y. Gao, J. B. Dickerson, F. Guo, J. Zheng, Y. Zheng, Rational design and characterization of a Rac GTPase-specific small molecule inhibitor. *Proc. Natl. Acad. Sci. U.S.A.* **101**, 7618–7623 (2004).
38. P. Sander *et al*., Vacquinol-1-inducible cell death in glioblastoma multiforme is counter-regulated by TRPM7 activity induced by exogenous ATP. *Oncotarget* **8**, 35124–35137 (2017).
39. Y. Son *et al*., Mitogen-activated protein kinases and reactive oxygen species: How can ROS activate MAPK pathways? *J. Signal Transduct.* **2011**, 792639 (2011).
40. D. O. Walterhouse *et al*., Reduction of cyclophosphamide dose for patients with subset 2 low-risk rhabdomyosarcoma is associated with an increased risk of recurrence: A report from the Soft Tissue Sarcoma Committee of the Children's Oncology Group. *Cancer* **123**, 2368–2375 (2017).
41. S. Malempati, D. S. Hawkins, Rhabdomyosarcoma: Review of the Children's Oncology Group (COG) Soft-Tissue Sarcoma Committee experience and rationale for current COG studies. *Pediatr. Blood Cancer* **59**, 5–10 (2012).
42. P. Gulhati *et al*., mTORC1 and mTORC2 regulate EMT, motility, and metastasis of colorectal cancer via RhoA and Rac1 signaling pathways. *Cancer Res.* **71**, 3246–3256 (2011).
43. M. Laplante, D. M. Sabatini, mTOR signaling in growth control and disease. *Cell* **149**, 274–293 (2012).
44. H. Lee, Phosphorylated mTOR expression profiles in human normal and carcinoma tissues. *Dis. Markers* **2017**, 1397063 (2017).
45. P. Liu, H. Cheng, T. M. Roberts, J. J. Zhao, Targeting the phosphoinositide 3-kinase pathway in cancer. *Nat. Rev. Drug Discov.* **8**, 627–644 (2009).
46. S. M. Johnson *et al*., Novel expression patterns of PI3K/Akt/mTOR signaling pathway components in colorectal cancer. *J. Am. Coll. Surg.* **210**, 767–776, 776–8 (2010).
47. M. Razmara, C. H. Heldin, J. Lennartsson, Platelet-derived growth factor-induced Akt phosphorylation requires mTOR/Rictor and phospholipase C-γ1, whereas S6 phosphorylation depends on mTOR/Raptor and phospholipase D. *Cell Commun. Signal.* **11**, 3 (2013).
48. Q. W. Fan *et al*., EGFR signals to mTOR through PKC and independently of Akt in glioma. *Sci. Signal.* **2**, ra4 (2009).
49. D. D. Sarbassov, D. A. Guertin, S. M. Ali, D. M. Sabatini, Phosphorylation and regulation of Akt/PKB by the rictor-mTOR complex. *Science* **307**, 1098–1101 (2005).
50. D. R. Alessi, L. R. Pearce, J. M. García-Martínez, New insights into mTOR signaling: mTORC2 and beyond. *Sci. Signal.* **2**, pe27 (2009).
51. G. Yang, D. S. Murashige, S. J. Humphrey, D. E. James, A positive feedback loop between Akt and mTORC2 via SIN1 phosphorylation. *Cell Rep.* **12**, 937–943 (2015).
52. Q. Li, X. M. Song, Y. Y. Ji, H. Jiang, L. G. Xu, The dual mTORC1 and mTORC2 inhibitor AZD8055 inhibits head and neck squamous cell carcinoma cell growth in vivo and in vitro. *Biochem. Biophys. Res. Commun.* **440**, 701–706 (2013).
53. K. Petrossian *et al*., Use of dual mTOR inhibitor MLN0128 against everolimus-resistant breast cancer. *Breast Cancer Res. Treat.* **170**, 499–506 (2018).
54. N. E. Mbah, J. H. Overmeyer, W. A. Maltese, Disruption of endolysosomal trafficking pathways in glioma cells by methuosis-inducing indole-based chalcones. *Cell Biol. Toxicol.* **33**, 263–282 (2017).
55. X. Gong *et al*., Tubeimoside 1 acts as a chemotherapeutic synergist via stimulating macropinocytosis. *Front. Pharmacol.* **9**, 1044 (2018).
56. H. Zhou, S. Huang, Role of mTOR signaling in tumor cell motility, invasion and metastasis. *Curr. Protein Pept. Sci.* **12**, 30–42 (2011).
57. F. Zhang *et al*., mTOR complex component Rictor interacts with PKCzeta and regulates cancer cell metastasis. *Cancer Res.* **70**, 9360–9370 (2010).
58. H. Yamaguchi, J. Condeelis, Regulation of the actin cytoskeleton in cancer cell migration and invasion. *Biochim. Biophys. Acta* **1773**, 642–652 (2007).
59. Z. Erami *et al*., Rac1-stimulated macropinocytosis enhances Gβγ activation of PI3Kβ. *Biochem. J.* **474**, 3903–3914 (2017).
60. D. Xia *et al*., Mitogen-activated protein kinase kinase-4 promotes cell survival by decreasing PTEN expression through an NF kappa B-dependent pathway. *J. Biol. Chem.* **282**, 3507–3519 (2007).
61. N. Tejeda-Muñoz, L. V. Albrecht, M. H. Bui, E. M. De Robertis, Wnt canonical pathway activates macropinocytosis and lysosomal degradation of extracellular proteins. *Proc. Natl. Acad. Sci. U.S.A.* **116**, 10402–10411 (2019).